Simultaneous 3D whole-heart bright-blood and black blood imaging for cardiovascular anatomy and wall assessment with interleaved T2prep-IR

Journal:	*Magnetic Resonance in Medicine*
Manuscript ID	MRM-18-19461.R2
Wiley - Manuscript type:	Full Paper
Date Submitted by the Author:	19-Feb-2019
Complete List of Authors:	Milotta, Giorgia; King's College London Division of Imaging Sciences and Biomedical Engineering Ginami, Giulia; King's College London, Imaging Sciences Division, Biomedical Engineering Dept. Lima da Cruz, Gastão; King's College London, Imaging Sciences & Biomedical Engineering Neji, Radhouene; St Thomas' Hospital, School of Biomedical Engineering and Imaging Sciences; Prieto, Claudia; King's College London, Interdisciplinary Medical Imaging Group Botnar, Rene; King's College London, Imaging Sciences Division;
Research Type:	Technique Development < Technical Research, Pulse sequence design < Technique Development < Technical Research
Research Focus:	Anatomy < Heart < Cardiovascular, Anatomy < Vasculature < Cardiovascular
Note: The following files were submitted by the author for peer review, but cannot be converted to PDF. You must view these files (e.g. movies) online.	
Supporting information video S1.gif Supporting information video S2.gif	

Simultaneous 3D whole-heart bright-blood and black blood imaging for cardiovascular anatomy and wall assessment with interleaved T2prep-IR

Giorgia Milotta[1], Giulia Ginami[1], Gastao Cruz[1], Radhouene Neji[1, 2], Claudia Prieto[1, 3], René M. Botnar[1, 3]

Affiliations:

1. School of Biomedical Engineering and Imaging Sciences, King's College London, London, United Kingdom.
2. MR Research Collaborations, Siemens Healthcare Limited, Frimley, United Kingdom.
3. Escuela de Ingeniería, Pontificia Universidad Católica de Chile, Santiago, Chile.

Word count: ~ 5000 words (plus 250 words for the Abstract).

Correspondence to: Giorgia Milotta, School of Biomedical Engineering and Imaging Sciences, St Thomas' Hospital (3rd Floor - Lambeth Wing), Westminster Bridge Rd, London SE1 7EH – UK. E-mail: giorgia.milotta@kcl.ac.uk

ABSTRACT

Purpose: To develop a motion corrected 3D flow-insensitive imaging approach (iT2prep-IR) for simultaneous lumen and wall visualization of the great thoracic vessels and cardiac structures.

Methods: A 3D flow-insensitive approach for simultaneous cardiovascular lumen and wall visualization (iT2prep) has been previously proposed. This approach requires subject-dependent weighted subtraction to completely null the arterial blood signal in the black-blood volume. Here we propose an interleaved T2 prepared-Inversion Recovery (T2prep-IR) approach to improve wall visualization and remove need for weighted subtraction. The proposed sequence is based on the acquisition and direct subtraction of two interleaved 3D whole-heart datasets acquired with and without T2prep-IR preparation. Image navigators are acquired prior to data acquisition to enable 2D translational and 3D non-rigid motion correction allowing 100% respiratory scan efficiency. The proposed approach was evaluated in 10 healthy subjects and compared with the conventional 2D double inversion recovery (DIR) sequence and the 3D iT2prep sequence. Additionally, five patients with congenital heart disease were acquired to test the clinical feasibility of the proposed approach.

Results: The proposed iT2prep-IR sequence showed improved blood nulling compared to both DIR and iT2prep techniques in terms of signal-to-noise-ratio (SNR_{blood} = 6.9, 12.2 and 18.2 respectively) and contrast-to-noise-ratio ($CNR_{myoc-blood}$ = 28.4, 15.4 and 15.3 respectively). No statistical difference was observed between iT2prep-IR, iT2prep and DIR atrial and ventricular wall thickness quantification.

Conclusion: The proposed interleaved T2prep-IR sequence enables the simultaneous lumen and wall visualization of cardiac structures and shows promising results in terms of SNR, CNR and wall thickness measurement.

Keywords: 3D whole-heart, bright-blood cardiac anatomy, black-blood vessel wall, black-blood atrial wall, respiratory motion correction, interleaved T2prep-IR.

Introduction

Visualization of cardiovascular anatomy is important for diagnosis, risk stratification and planning of interventional procedures both in patients with congenital and non-congenital heart disease. Cardiac magnetic resonance imaging (MRI) plays an important role in the investigation and follow up of patients with such diseases [1]–[3]. Particularly bright-blood and black-blood imaging can be complementarily used for lumen and wall visualization of the great thoracic vessels and cardiac structures.

3D whole-heart bright-blood MRI enables the visualization of cardiac structures, great thoracic vessels and coronary arteries. Data acquisition is commonly synchronized with patient's ECG to minimize cardiac motion [4], whereas respiratory motion is usually minimized using 1D diaphragmatic navigators to gate the acquisition to end-expiration and correct for superior-inferior respiratory motion [5]. However, 1D respiratory navigator gating leads to long and unpredictable scan times since data acquired outside of the gating window need to be re-acquired. In the last decade several self-navigated and image-based navigator techniques have been proposed and employed to achieve 100% respiratory scan efficiency and thus lead to shorter and more predictable scan times [6]–[11].

Black-blood MRI has been successfully used for vessel wall visualization in the aorta, carotid, and coronary arteries [12]–[15]. Black-blood imaging of the cardiovascular structures (myocardial and vessel walls) is challenging due to respiratory and cardiac motion, in particular for thin structures such as left and right atrium (thickness ranging between 2-3mm [16] and 3-4mm [17] respectively). Thus, high spatial resolution and motion compensation techniques are required. Similarly to the 3D bright-blood approaches cardiac motion is minimized by synchronizing the acquisition with patient's ECG, whereas respiratory motion is usually minimized by performing the acquisition under breath-hold

(2D imaging) or utilizing prospective 1D diaphragmatic navigator gating and correction (3D imaging). Conventional 2D black-blood double inversion recovery (DIR) imaging techniques rely on blood flow [13]–[15], which can be insufficient to obtain good quality images in patients with slow or in-plane (e.g. 2, 3 and 4 chamber view) blood flow. Furthermore, this sequence provides limited coverage, requires sophisticated acquisition planning [18] and is challenging to extend to 3D.

An alternative motion-sensitized driven equilibrium (MSDE) black-blood sequence, has been successfully used for carotid, aortic and cardiac wall imaging [19]–[21]. MSDE relies on gradients to dephase moving spins and thus to null blood signal [22]. MSDE is not limited by low inflow or slow flow, however high first-order momentum dephasing gradients are necessary to null the blood signal [23]. Therefore, blood nulling of complex flow-patterns, such as the ones present in the cardiac chambers, could be challenging and gradient amplitude and direction have to be optimized on a specific patient level.

Flow-insensitive vessel wall imaging techniques have been proposed to overcome this limitation. A T2-preparation pulse (T2prep) was combined with a non-selective inversion recovery (IR) pulse (T2prep-IR) to suppress blood signal and maintain vessel wall signal in 2D spin-echo aortic and carotid wall imaging [24]. However, this technique achieves relatively low signal from tissues with short T2 values such as myocardium and vessel walls. It has been shown that the acquisition of two datasets with and without T2preparation pulses allowed the suppression of arterial blood and visualization of deoxygenated venous blood [25]. Andia et al. [26] extended this T2prep subtraction technique and proposed an alternative flow-insensitive free-breathing 3D whole-heart vessel wall imaging technique that takes advantage of the shorter T2 relaxation time of the myocardium and vessel wall with respect to blood. With this approach two interleaved datasets are acquired with and without T2prep. The weighted subtraction of the two acquired datasets allows suppression of the blood signal while maintaining high tissue signal, allowing good delineation of the aortic and coronary artery walls. This weighted subtraction however is subject-dependent,

thus limiting the applicability of the method. Moreover, in [26] an interleaved dual-gated acquisition was performed to reduce motion sensitivity in the subtracted image, however respiratory dual-gating with 1D diaphragmatic navigator lead to excessively long acquisition times.

In this work, we propose a new robust approach for 3D flow-insensitive vessel wall imaging that aims to improve the previously developed interleaved T2prep (iT2prep) acquisition by: a) improving vessel wall to blood contrast, and b) removing the need of weighting subtraction. Additionally, acquisition time will be reduced by employing image based navigation (iNAV) [8] in concert with non-rigid respiratory motion correction with near 100% scan efficiency as proposed in a recent work [10]. Similar to the previously proposed iT2prep, our approach simultaneously provides a bright-blood volume for fully co-registered cardiac anatomy and great vessel lumen visualization.

The proposed technique is based on the acquisition and subtraction of two interleaved balanced steady-state free precession (bSSFP) volumes. The first dataset is obtained by applying a T2prep-IR pulse prior to data acquisition, whereas the second dataset is obtained without preparation pulses. The combination of T2prep and IR pulses enhances the myocardium signal after the subtraction and improves nulling of the blood signal potentially removing the necessity to perform a weighted subtraction between the two acquired volumes. Image navigators are acquired prior to each data acquisition to enable 2D translational and 3D non-rigid motion correction with near 100% respiratory scan efficiency and predictable scan time.

Methods

Framework

A 3D whole-heart, ECG triggered, vessel wall imaging sequence was implemented to enable non-rigid respiratory motion corrected iT2prep-IR acquisition as shown in Figure 1.

The proposed iT2prep-IR sequence acquires two 3D whole-heart ECG-triggered bSSFP bright-blood volumes with a spiral profile order Cartesian trajectory [27] in an interleaved fashion. The first bright-blood volume is acquired with a T2prep-IR preparation to optimize contrast between myocardium and arterial blood (odd dataset, lumen and cardiac anatomy visualization). The second bright-blood dataset is acquired with no preparation pulses (even dataset). Fat suppression is achieved in the odd dataset with a short inversion time (TI) IR approach [28], whereas spectral pre-saturation [29] is exploited to suppress fat in the even dataset.

2D low-resolution image based navigators (iNAVs) [8] are acquired in each heartbeat prior to imaging to estimate and correct for superior-inferior (SI) and left-right (LR) beat-to-beat translational respiratory motion without any data rejection. Furthermore, 3D bin-to-bin non-rigid respiratory motion correction is performed on each bright-blood dataset [10] using the general matrix description reconstruction [30] and 3D non-rigid image registration [31] is performed between the two bright-blood datasets prior to subtraction to generate the black-blood image of the cardiovascular structures and walls.

Respiratory motion correction is briefly described hereafter. 2D translational motion detection is achieved by manually selecting a region of interest (ROI), corresponding to the iNAV, around the heart during acquisition planning. A template-matching algorithm exploiting mutual information [32] is used to estimate the SI and LR beat-to-beat translational motion. Data with SI motion estimation falling outside the interval calculated as mean ± 2 times standard deviation are considered outliers due to deep breathing and are removed. The so obtained translational respiratory motion corrected acquisition is rescaled exploiting a gradient entropy autofocusing technique [33], [34] to account for any errors in translational motion estimation due to reduced contrast in the even datasets. The estimated SI displacement is used to bin the acquired data into different respiratory positions within the breathing cycle. 2D translational intra-bin motion correction is performed as a linear phase shift in k-space using the estimated SI and LR displacements [35]. Each bin is

reconstructed using a soft-gated iterative SENSE approach [36], [37] and 3D non-rigid inter-bin motion estimation is performed via image registration using the end-expiration bin as reference [32]. The estimated 3D non-rigid deformation fields are incorporated in a general matrix description reconstruction [30].

Simulations

Extended phase graph (EPG) [38] simulations were performed to analyze the longitudinal magnetization behaviour of myocardium and arterial blood for different combinations of T2prep length, TI and acquisition parameters of the proposed iT2prep-IR sequence. Additionally, EPG simulations were performed to investigate if the T2prep-IR module order (T2prep-IR or IR-T2prep) would affect the magnetization of blood and myocardium in odd, even and subtracted datasets. Since no significant difference was observed between the two approaches (Supporting Information Figure 1), the T2prep-IR configuration was employed for the preparation module.

Simulations were performed with the following tissues parameters: myocardium T_1= 1100ms and T_2= 50ms, arterial blood T_1 =1500ms and T_2 = 300ms. T1 and T2 values of both myocardium and blood were set to match the values of a standardized T_1/ T_2 phantom described in [39].

Image acquisition was simulated for a centric reordering bSSFP sequence composed of 14 ramp-up pulses corresponding to the iNAV and 33 k-space lines per heartbeat, corresponding to an acquisition window of 120ms. The parameters considered in the simulation included: TR = 3.6ms, flip angle of 90degrees in both odd and even acquisitions and heart rate of 45bpm. Inversion time was set to 110ms to suppress the signal from epicardial fat in odd heartbeats. The effect of different T2prep lengths on blood and vessel wall signal was investigated by computing the steady state magnetization in the centre of the k-space in odd and even heartbeats. Additionally, EPG simulations results obtained for

45bpm, 70bpm and 100bpm with iT2prep and the proposed iT2prep-IR sequence were compared.

Data acquisition – healthy subjects

Data were acquired in 10 healthy subjects (32.9±8.2 years, 5 males) with the proposed iT2prep-IR, the iT2prep, and DIR technique for comparison purposes on a 1.5T MR scanner (MAGNETON Aera, Siemens Healthcare, Erlangen, Germany). Written informed consent was obtained from all participants before undergoing the MR scans and the study was approved by the Institutional Review Board.

Data were acquired with an 18-channel chest coil and a 32-channel spinal coil. iT2prep-IR imaging parameters were set as follow: coronal orientation, isotropic spatial resolution 1.4x1.4x1.4mm^3, field of view (FOV) = 320x320x80-105mm, bandwidth= 1165Hz/pixel, repetition time (TR) = 3.6ms, echo time (TE) = 1.5ms, flip angle = 90degrees, 14 bSSFP ramp-up pulses leading to an iNAV resolution of 1.4x22.8mm interpolated to 1.4x1.4mm before motion estimation, T2prep = 40ms, TI = 110ms, total acquisition time = 17min for fully sampled scans for a heart rate of 70 bpm. Matching imaging parameters were used for the iT2prep acquisition, whereas 2D DIR imaging parameters were: transversal orientation, in-plane resolution = 1.4x1.4mm, slice thickness = 7mm, gradient echo acquisition with flip angle of 15degrees, TE/TR=2.35/5ms, bandwidth = 437Hz/pixel and breath hold duration = 20sec. Image acquisition was ECG-triggered and performed during diastolic quiescent period. A high resolution 2D CINE was acquired prior to data acquisition to determine the subject-specific trigger delay and acquisition window, ranging from 100 to 120ms.

Data acquisition – patients

Data were acquired in 5 patients (43±14.2 years, 4 males) with congenital heart disease in a proof of concept study to test the feasibility of the proposed iT2prep-IR approach. Written informed consent was obtained from all participants before undergoing the MR scans and the study was approved by the Institutional Review Board.

Data were acquired with the same imaging parameters used for the healthy subjects: coronal orientation with isotropic resolution of 1.4mm^3, FOV=320x320x90-115mm, bandwidth= 1165 Hz/pixel, TR/TE = 3.6/1.5ms, flip angle = 90degrees, 14 bSSFP ramp-up for iNAV acquisition, T2prep duration = 40ms, TI = 110ms. Patients heart rate was 70.8±5.97 bmp (range 62-78 bpm) and a patient specific trigger delay coinciding with mid-diastolic resting period (80-95ms acquisition window) was chosen. Different to the healthy subjects study an acceleration factor of 2 was used to accelerate the scan.

Image reconstruction

Raw data were exported from the scanner and reconstructed in MATLAB (The MathWorks, Inc., Natick, MA, USA). For both the proposed iT2prep-IR and iT2prep sequences odd and even datasets were independently reconstructed. As first step translational motion correction to end-expiration and autofocus motion correction were performed, as previously described. Respiratory motion autofocusing scaling factors for odd and even dataset ranged between 0.7-1 and 0.5-0.7 respectively. The rescaled motion estimation curves were used to bin the data in different respiratory phases. Approximately 4-5 equally populated bins were reconstructed with a maximum bin size of 4.0 mm for each dataset, leading to undersampling factors of ~4-5 for each bin for the healthy subject study and of ~8-10 for each bin for the patient study, and 5 iterations were used for the soft-gated, respiratory resolved iterative SENSE reconstruction. Non-rigid motion fields were obtained by non-rigid registration with the end-expiratory bin. Finally, the previously described general matrix description motion corrected reconstruction was performed to obtain the non-rigid motion corrected volumes. Image trilinear interpolation (reconstructed isotropic resolution of 0.6x0.6x0.6mm^3) and registration were performed prior direct subtraction to obtain the iT2prep-IR black-blood volume, whereas subject-specific thresholding and weighted subtraction was needed to obtain the iT2prep black-blood volume.

The clinical DIR sequence was reconstructed using the scanner software (Syngo MR E11A, Siemens Healthcare, Erlangen, Germany). Image linear interpolation was performed to obtain an in-plane resolution of 0.6x0.6mm.

Data analysis

All quantitative data analysis was performed on the healthy subjects data, while patient data were assessed in terms of visual image quality.

The proposed iT2prep-IR sequence was compared to iT2prep and DIR in terms of signal-to-noise ratio (SNR), contrast-to-noise ratio (CNR) and myocardial wall thickness of the left ventricle (LV), left atrium (LA), right ventricle (RV) and right atrium (RA). Specifically, SNR_{blood}, SNR_{myoc} and $CNR_{myoc\text{-}blood}$ were computed for iT2prep-IR, iT2prep and DIR black-blood volumes. iT2prep-IR and iT2prep bright-blood volumes were compared in terms of SNR_{blood}, SNR_{myoc} and $CNR_{blood\text{-}myoc}$.

Measurements of myocardial wall thickness were performed on the black-blood iT2prep-IR, iT2prep and DIR datasets. Wall thickness was quantified using Soap-Bubble software [40] in four-chamber views generated using OsiriX software (version MD 9.5), a linear interpolation was selected to rotate the datasets in OsiriX.

Statistical significance for all quantitative endpoints was assessed using a paired two-tailed Student t-test with Bonferroni correction for multiple comparisons. P value < 0.05 was considered as statistically significant.

Results

All simulations, data acquisition and reconstructions were carried out successfully and results are reported hereafter.

Simulations

A simulation of myocardium and blood steady-state magnetization of the proposed iT2prep-IR sequence as a function of T2prep duration is shown in Figure 2. The steady state magnetization was measured at the beginning of the acquisition for both odd and even heartbeats (M_A and M_B respectively) which coincides with the k-space centre, containing contrast information, as data acquisition was simulated with centric reordering. The purpose

of applying a T2prep-IR pulse module is to minimize the vascular and myocardial wall signal in odd heartbeats in order to enhance vessel wall and myocardium in the subtracted dataset and to obtain similar arterial blood signals in odd and even datasets in order to null blood in the direct subtraction (without need of weighting). In addition, the T2prep-IR acquisition (odd heartbeat) was designed to obtain a bright-blood whole heart dataset for visualization of cardiac anatomy and great vessels.

For simulations at a heart rate of 45bpm a T2prep of 40ms was selected as a good compromise between blood nulling in the black-blood volume and blood to myocardium contrast in the anatomical bright-blood dataset. T2prep length of 40ms leads to a myocardium magnetization M_z/M_0 of 0.061 in odd heartbeats and 0.369 in even heartbeats, whereas the blood magnetization was 0.266 and 0.303 in odd and even datasets respectively. This results in an expected blood-myocardium ratio of 4.36 in the bright-blood dataset. On the other hand, myocardium and blood magnetizations of 0.308 and 0.037 in the subtracted dataset were obtained, leading to a myocardium-blood magnetization difference of 0.268 and myocardium-blood ratio equal to 8.31.

iT2prep-IR and iT2prep magnetization evolutions are compared in Figure 3. Odd and even iT2prep myocardium signals were 0.199 and 0.413 respectively, whereas odd and even blood magnetization was measured to be 0.439 and 0.486 respectively. Blood-myocardium ratio of the bright-blood dataset was 2.31 leading to similar but slightly lower $CNR_{blood\text{-}myoc}$ as in the proposed sequence. Myocardium and blood magnetization in the direct subtracted dataset are 0.214 and 0.047 M_z/M_0, resulting in a myocardium-blood ratio of 4.56, which is significantly lower than for the proposed iT2prep-IR sequence. Blood nulling and myocardium-blood ratio of subtracted dataset were computed also for faster (70bpm and 100bpm) heart rates (Figure 4). For all simulated heart rates the proposed sequence shows better blood nulling properties compared to iT2prep (iT2prep-IR 45bpm - 70bpm - 100bpm = 0.037, 0.034 and 0.033 M_z/M_0 vs iT2prep 45bpm - 70bpm - 100bpm = 0.047, 0.067 and 0.080 M_z/M_0) and higher myocardium-blood ratio (8.13 - 6.91 - 5.79 obtained with iT2prep-

IR vs 4.56 - 2.46 - 1.47 with iT2prep for 45,70 and 100bpm respectively). The iT2prep-IR sequence is therefore expected to better null the blood signal with no need for weighted subtraction in concert with an increase in $CNR_{myoc-blood}$ in the black-blood volume.

Healthy subjects

iT2prep-IR and iT2prep fully sampled free breathing acquisitions were successfully carried out for all subjects with nominal acquisition time of 17.0±1.3min. 2D image navigation and 3D non-rigid motion correction allowed near 100% scan efficiency and only outliers due to deep breaths were discarded in the reconstruction process. Four 2D DIR breath hold acquisitions were performed for each subject at different transversal slice locations with nominal acquisition time of 18-22 sec per slice and ~15-20 sec recovery period between breath holds.

Coronal and transversal views of two representative healthy subjects acquired with the proposed iT2prep-IR sequence are shown in Figure 5. The first column shows the bright-blood anatomical images for each subject whereas the second column shows the corresponding black-blood images. The proposed approach allows to suppress blood signal after direct subtraction in all the heart chambers allowing the visualization of LA, RA, RV and LV walls as well as papillary muscles and aortic wall. Additionally, two Supporting Information Videos S1 and S2 show the bright-blood and co-registered black-blood 3D volumes for one representative healthy subject. Mostly uniform blood suppression is obtained in all the cardiac chambers.

Comparison between black-blood volumes acquired with the proposed iT2prep-IR sequence, with iT2prep and DIR acquisitions has been performed (Figure 6a). Residual blood signal is present in the DIR acquisitions due to slow or in-plane blood flow, thus affecting wall visualization. After subject-dependent weighted subtraction, iT2prep improves nulling of the blood signal compared to DIR, however blood suppression is not uniform across all heart chambers and some residual blood signal is present especially in

the right side of the heart. Additionally, the corresponding bright-blood volumes acquired with iT2prep and iT2prep-IR were compared (Figure 6b). The two sequences show similar contrast and excellent anatomical visualization of the heart chambers and aorta. SNR of blood and myocardium were computed for black-blood and bright-blood volumes acquired for all subjects, additionally $CNR_{myoc\text{-}blood}$ and $CNR_{blood\text{-}myoc}$ were calculated for black and bright volumes respectively (Figure 7). Black-blood images acquired with the iT2prep-IR sequence showed a significantly higher SNR_{myoc} compared to both iT2prep ($p<0.05$) and DIR ($p<0.001$), SNR_{blood} was lower compared to iT2prep and DIR but no statistical difference was observed. $CNR_{myoc\text{-}blood}$ was increased with the proposed approach and statistical difference was observed compared to iT2prep dataset obtained after direct subtraction and DIR ($p<0.05$).

The comparison carried out between iT2prep and iT2prep-IR bright-blood volumes did not show any statistical difference between computed SNR_{myoc}, SNR_{blood} and $CNR_{blood\text{-}myoc}$, however a consistent trend of higher $CNR_{blood\text{-}myoc}$ was observed for the proposed technique. iT2prep-IR was compared to iT2prep and DIR in terms of myocardium wall thickness quantification. LV, RV, RA and LA wall thickness measurements were successfully obtained for all subjects. iT2prep-IR wall thickness was measured to be 2.99±0.2mm, 9.51±1.67mm, 2.91±0.32mm and 3.2±0.44mm respectively for LA, LV, RA and RV and good agreement was found with the physiological range of myocardium wall thickness reported in the literature [16], [17], [41], [42]. No statistical difference was observed with iT2prep measurements (LA=2.92±0.38mm, LV=9.33±1.82mm, RA=2.70±0.19mm, RV=3.14±0.36mm). DIR technique globally overestimated the wall thickness (LA=3.19±0.34mm, LV=11.16±2.19mm, RA=3.79±0.24mm, RV=3.71±0.29), however statistical difference ($p<0.05$) was observed only for LV.

Patients

iT2prep-IR 2-fold undersampled free breathing acquisitions were successfully carried out for all subjects with nominal acquisition time of 9min±52sec. Coronal and transversal views

of three representative patients are shown in Figure 8. Corresponding bright-blood and black-blood volumes are shown respectively in the first and second column for each patient. Good blood signal suppression was achieved, with some residual blood signal present in the LA. An overall good image quality was obtained with RA, RV, LA and LA walls being visible.

Discussion

In this study, a novel 3D flow-insensitive motion corrected sequence for simultaneous lumen (bright-blood volume) and vessel wall (black-blood volume) visualization of the great thoracic vessels and cardiac structures was proposed. This approach is based on the acquisition of two bright-blood whole-heart interleaved datasets: one with T2prep-IR preparation (odd heartbeats) and one without preparation pulses (even heartbeats). The black-blood dataset is obtained by performing a direct subtraction between the even and the odd volumes. When compared to the previously published flow-insensitive iT2prep approach [26], the proposed technique does not require a weighted subtraction between the two datasets to null the blood signal. The weighting factor used by Andia et al. was subject specific, depending on the heart rate frequency and on the acquisition protocol; thus, the approach proposed here should be more robust to inter-subject variability.

2D image-based navigation was integrated with the iT2prep-IR framework to enable 2D translational and 3D non-rigid motion correction with 100% respiratory scan efficiency and predictable scan time. iNAVs acquisition preceded each bright-blood dataset and motion correction was performed for the two volumes independently. The enhanced contrast in odd heartbeats enabled better motion estimation with respect to the even dataset. Conversely, the lower contrast of even iNAVs' lead to sub-optimal translational motion estimation and correction. A gradient entropy based autofocusing technique was therefore used to rescale the originally estimated translational motion curves. This added step ensured an improved motion estimation also in case of low contrast iNAV acquisitions thus reducing motion

artefacts in each respiratory bin and consequently improving the non-rigid motion estimation and correction.

Extended phase graph simulations were carried out to optimize the acquisition parameters. A T2prep of 40ms was found to be a good compromise to null the blood signal in the subtracted dataset and myocardium signal in odd datasets, while preserving the blood magnetization in the bright-blood dataset. This parameter setting enhanced the myocardium-to-blood contrast in the subtracted volume and the blood-to-myocardium contrast in bright-blood volume. Myocardium to blood ratio heart rate dependency may be explained due to a reduction in recovery time between dataset acquisitions, resulting in insufficient magnetization recovery prior to subsequent inversion pulse which will reduce the myocardium magnetization steady state thus affecting contrast between myocardium and blood.

Magnetization evolution of the proposed iT2prep-IR sequence and of the previously proposed iT2prep sequence were compared and SNR and CNR were computed for both bright-blood and black-blood datasets. The proposed iT2prep-IR sequence provided increased SNR_{myoc} and $CNR_{myoc\text{-}blood}$ in the black-blood volume obtained after direct subtraction, compared to the iT2prep approach, for both slow and fast heart rates. Myocardium to blood ratio heart rate dependency may be explained due to a reduction in recovery time between dataset acquisitions, resulting in insufficient magnetization recovery prior to subsequent inversion pulse which will reduce the myocardium magnetization steady state thus affecting contrast between myocardium and blood. Higher SNR_{blood} and similar $CNR_{blood\text{-}myoc}$ were observed in the odd dataset (lumen and cardiac structure visualization).

SNR and CNR quantification from volunteer scans were in good agreement with simulation results. iT2prep-IR black-blood volume showed higher SNR_{myoc} and $CNR_{myoc\text{-}blood}$ compared to weighted subtraction obtained with iT2prep and to DIR acquisitions. No

statistical difference was observed between SNR_{blood} and $CNR_{blood-myoc}$ of bright-blood iT2prep-IR and iT2prep acquisitions.

iT2prep-IR black-blood volume showed better nulling of blood signal across all cardiac chambers compared to iT2prep and DIR. Residual blood signal due to slow flow was observed in DIR acquisitions, especially in areas in which the flow is not perpendicular to the acquisition plane (such as the atria). Residual blood signal was also observed in the black-blood iT2prep acquisitions after weighted subtraction, especially in the right side of the heart. This non uniform nulling could be explained by the presence of venous blood in the right part of the heart, which has a lower T2 than arterial blood. The proposed technique exploits the combination of a T2prep and an IR to generate a mixed T1/T2 contrast thus allowing a better blood nulling in all the cardiac chambers. The proposed sequence improves blood signal nulling compared to DIR and iT2prep sequences, however some residual blood signal due to slow flow was observed particularly in the left atrium. Residual blood signal may be explained due to suboptimal shimming. A sub-optimal shim leads to B_0 inhomogeneities (and can be understood as a local small time-invariant background gradient) that may affect the T2prep pre-pulse leading to residual blood signal in the subtracted volume. A possible solution would be to replace the T2prep with a MTC preparation pulse in order to minimize dependency on B_0 inhomogeneities and this will be investigated in future studies.

iT2prep-IR, iT2prep and DIR sequences were also compared with respect to the assessment of myocardial and atrial wall thickness (LV, LA, RV and RA). A general wall thickness overestimation was observed with DIR in all volunteers. This overestimation, previously reported in the literature for [43], could be a consequence of the higher slice thickness (7mm compared to 1.4mm of iT2prep-IR and iT2prep) necessary to achieve sufficient SNR with the 2D acquisition and/or a result of bright signal from slow flowing blood. However, a significant statistical difference was observed only for the LV measurement ($p<0.005$). Similar wall thickness measurements were obtained with iT2prep and the proposed

iT2prep-IR sequence. However, in 2 healthy subjects measurement of the RA wall thickness in the iT2prep black-blood volume was limited to the posterior atrial wall due to residual blood signal adjacent to the anterior atrial wall. Wall thickness measurements in iT2prep-IR datasets were successful in all healthy subjects.

Underestimation of myocardium wall thickness in the subtracted dataset may also be explained due to partial volume artefacts between myocardium and blood, particularly in case of residual blurring due to motion. The proposed approach aims to minimize motion artefacts by performing an independent non-rigid motion correction on both acquired datasets followed by non-rigid registration between the two datasets. Thus, reducing partial volume artefacts in pixels at blood-myocardium interface (0.6mm^2 after interpolation). Despite the motion correction and registration described above, underestimation of thin structures (e.g. right ventricular wall thickness) may still occur due to residual partial volume effects, however these effects should be limited to the reconstructed spatial resolution and registration accuracy. Additionally, since no statistical difference was observed between the wall thickness measured with the proposed iT2prep-IR sequence and the thickness measured with the DIR approach we expect a minimal underestimation with respect to the true thickness.

Accurate motion correction and non-rigid registration between datasets is necessary not only to minimize partial volume artefacts, but also in order to visualize well delineated atria and ventricular walls in the subtracted volume. Indeed, any residual motion artefacts present in odd or even datasets would propagate into the black-blood volume leading to blurring of those structures. Additionally, mis-registration between datasets could generate signal voids in the atrial and ventricular wall due to subtraction of high blood signal in the odd dataset from myocardium signal in even dataset, whereas enhancement of blood signal could be visible in the proximity of cardiac walls due to the subtraction of myocardium from blood signal in odd and even datasets respectively. Another limitation of the current work is the long acquisition time of ~17min for fully sampled scans as two high-resolution

volumes need to be acquired. This sequence enables to obtain a black-blood and a bright-blood cardiac volume simultaneously, thereby providing complementary diagnostic information, at the expense of a prolonged acquisition time. Fully sampled acquisitions were considered in this proof-of-concept study for the healthy subjects, however under-sampling reconstruction techniques as those in [44], [45] can be employed to accelerate the scan, further minimizing motion artefacts and facilitating clinical translation.

Five patients were acquired with the proposed iT2prep-IR sequence as a clinical proof of concept study. Good blood signal nulling was achieved, enabling the visualization of RA, RV, LA and LV walls in all patients. Some myocardial signal variations, due to residual undersampling and/or motion artefacts, are visible in the images acquired in patients. Acquisition in this case was performed with an undersampling factor of 2x, resulting in each respiratory bin being undersampled by a factor of 8-10x. Reconstruction was performed with an iterative SENSE approach, that may be resulting in some remaining aliasing artefacts. More advanced reconstruction methods [46] will be investigated in future studies.

An additional potential limitation of the proposed work is fat suppression. Fat magnetization before the application of fat suppression differs in odd and even datasets, therefore fat suppression is performed differently in the two datasets in order to individually null fat signal. In the bright-blood dataset epicardial fat suppression is achieved with a short inversion time IR (STIR) approach. The inversion pulse used in the T2prep-IR preparation module was exploited to null fat signal and an optimized inversion time of 110ms was chosen. In contrast, a spectral pre-saturation (SPIR) approach with a flip angle of 130deg was exploited to null fat signal in the even dataset. Both, the TI and SPIR flip angle were optimized to achieve optimal fat suppression for a heart rate of 60bpm. However, both the TI and SPIR flip angle selection are heart rate dependent and may lead to some residual fat signal in the subtracted dataset for lower or higher heart rates. Fat suppression may be

particularly challenging in patients with a large amount of epicardial fat, leading to partial volume effects and possible overestimation of the thickness of thin cardiac structures.

Conclusion

This work proposes a new flow-insensitive 3D whole-heart MRI sequence for simultaneous lumen and wall visualization of the great thoracic vessels and cardiac structures. The sequence is based on the acquisition of two differently weighted bright blood datasets preceded by 2D image-based navigation to ensure near 100% respiratory scan efficiency. The proposed iT2prep-IR sequence showed promising results in terms of blood signal nulling, SNR_{myoc} and $CNR_{myoc\text{-}blood}$ in healthy subjects without the need of weighted subtractions. The proposed framework was also tested on five patients, demonstrating consistent blood nulling in the cardiac chambers.

Acknowledgement

This work was supported by 1) the King's College London & Imperial College London EPSRC Centre for Doctoral Training in Medical Imaging (EP/L015226/1) and 2) EPSRC grants EP/P001009/1 and EP/P007619 and 3) the Wellcome EPSRC Centre for Medical Engineering (NS/A000049/1 and WT 203148/Z/16/Z)), and 4) the Department of Health via the National Institute for Health Research (NIHR) Cardiovascular Health Technology Cooperative (HTC) and comprehensive Biomedical Research Centre awarded to Guy's & St Thomas' NHS Foundation Trust in partnership with King's College London and King's College Hospital NHS Foundation Trust.

References

[1] S. Fratz *et al.*, "Guidelines and protocols for cardiovascular magnetic resonance in children and adults with congenital heart disease: SCMR expert consensus group on congenital heart disease," *J. Cardiovasc. Magn. Reson.*, vol. 15, no. 1, p. 51, 2013.

[2] F. Marcotte *et al.*, "Evaluation of Adult Congenital Heart Disease by Cardiac Magnetic Resonance Imaging," *Congenit. Heart Dis.*, vol. 4, no. 4, pp. 216–230,

2009.

[3] F. Bailliard, M. L. Hughes, and A. M. Taylor, "Introduction to cardiac imaging in infants and children: Techniques, potential, and role in the imaging work-up of various cardiac malformations and other pediatric heart conditions," *Eur. J. Radiol.*, vol. 68, no. 2, pp. 191–198, Nov. 2008.

[4] J. Felblinger, C. Lehmann, and C. Boesch, "Electrocardiogram acquisition during MR examinations for patient monitoring and sequence triggering," *Magn. Reson. Med.*, vol. 32, no. 4, 1994.

[5] R. L. Ehman and J. P. Felmlee, "Adaptive technique for high-definition MR imaging of moving structures.," *Radiology*, vol. 173, no. 1, pp. 255–263, Oct. 1989.

[6] C. Stehning, P. Börnert, K. Nehrke, H. Eggers, and M. Stuber, "Free-breathing whole-heart coronary MRA with 3D radial SSFP and self-navigated image reconstruction.," *Magn. Reson. Med.*, vol. 54, no. 2, pp. 476–80, Aug. 2005.

[7] D. Piccini, A. Littmann, S. Nielles-Vallespin, and M. O. Zenge, "Respiratory self-navigation for whole-heart bright-blood coronary MRI: Methods for robust isolation and automatic segmentation of the blood pool," *Magn. Reson. Med.*, vol. 68, no. 2, pp. 571–579, Dec. 2011.

[8] M. Henningsson, P. Koken, C. Stehning, R. Razavi, C. Prieto, and R. M. Botnar, "Whole-heart coronary MR angiography with 2D self-navigated image reconstruction," *Magn. Reson. Med.*, vol. 67, no. 2, 2012.

[9] J. Pang *et al.*, "Whole-heart coronary MRA with 100% respiratory gating efficiency: Self-navigated three-dimensional retrospective image-based motion correction (TRIM)," *Magn. Reson. Med.*, vol. 71, no. 1, pp. 67–74, Feb. 2013.

[10] G. Cruz, D. Atkinson, M. Henningsson, R. M. Botnar, and C. Prieto, "Highly efficient nonrigid motion-corrected 3D whole-heart coronary vessel wall imaging.," *Magn. Reson. Med.*, May 2016.

[11] J. Luo *et al.*, "Nonrigid Motion Correction with 3D Image-based Navigators for Coronary MR Angiography," *Magn. Reson. Med.*, vol. 77, no. 5, pp. 1884–1893, May 2017.

[12] C. Miao *et al.*, "Positive Remodeling of the Coronary Arteries Detected by Magnetic Resonance Imaging in an Asymptomatic Population: MESA (Multi-Ethnic Study of Atherosclerosis)," *J. Am. Coll. Cardiol.*, vol. 53, no. 18, pp. 1708–1715, 2009.

[13] S. D. Roes *et al.*, "Aortic vessel wall magnetic resonance imaging at 3.0 tesla: A reproducibility study of respiratory navigator gated free-breathing 3D black blood magnetic resonance imaging," *Magn. Reson. Med.*, vol. 61, no. 1, 2009.

[14] N. Balu, B. Chu, T. S. Hatsukami, C. Yuan, and V. L. Yarnykh, "Comparison between 2D and 3D high-resolution black-blood techniques for carotid artery wall imaging in clinically significant atherosclerosis," *J. Magn. Reson. Imaging*, vol. 27, no. 4, 2008.

[15] R. M. Botnar, W. Y. Kim, P. Börnert, M. Stuber, E. Spuentrup, and W. J. Manning, "3D coronary vessel wall imaging utilizing a local inversion technique with spiral image acquisition.," *Magn. Reson. Med.*, vol. 46, no. 5, pp. 848–54, Nov. 2001.

[16] K. TAKAHASHI *et al.*, "Relation Between Left Atrial Wall Thickness in Patients with Atrial Fibrillation and Intracardiac Electrogram Characteristics and ATP-Provoked Dormant Pulmonary Vein Conduction," *J. Cardiovasc. Electrophysiol.*, vol. 26, no. 6, pp. 597–605, Mar. 2015.

[17] M. Bishop *et al.*, "Three-dimensional atrial wall thickness maps to inform catheter ablation procedures for atrial fibrillation," *EP Eur.*, vol. 18, no. 3, pp. 376–383, Mar. 2016.

[18] G. Ginami, J. Yerly, P. G. Masci, and M. Stuber, "Golden angle dual-inversion recovery acquisition coupled with a flexible time-resolved sparse reconstruction facilitates sequence timing in high-resolution coronary vessel wall MRI at 3 T," *Magn. Reson. Med.*, vol. 77, no. 3, pp. 961–969, Feb. 2016.

[19] J. Wang, V. L. Yarnykh, and C. Yuan, "Enhanced image quality in black-blood MRI using the improved motion-sensitized driven-equilibrium (iMSDE) sequence," *J. Magn. Reson. Imaging*, vol. 31, no. 5, pp. 1256–1263, Apr. 2010.

[20] C. Zhu, M. J. Graves, J. Yuan, U. Sadat, J. H. Gillard, and A. J. Patterson,

"Optimization of Improved Motion-sensitized Driven-equilibrium (iMSDE) blood suppression for carotid artery wall imaging," *J. Cardiovasc. Magn. Reson.*, vol. 16, no. 1, p. 61, 2014.

[21] S. Srinivasan *et al.*, "Free-breathing 3D whole-heart black-blood imaging with motion sensitized driven equilibrium," *J. Magn. Reson. Imaging*, vol. 36, no. 2, pp. 379–386, Aug. 2012.

[22] I. Koktzoglou and D. Li, "Diffusion-prepared segmented steady-state free precession: Application to 3D black-blood cardiovascular magnetic resonance of the thoracic aorta and carotid artery walls," *J. Cardiovasc. Magn. Reson.*, vol. 9, no. 1, pp. 33–42, 2007.

[23] J. Wang, V. L. Yarnykh, T. Hatsukami, B. Chu, N. Balu, and C. Yuan, "Improved suppression of plaque-mimicking artifacts in black-blood carotid atherosclerosis imaging using a multislice motion-sensitized driven-equilibrium (MSDE) turbo spin-echo (TSE) sequence," *Magn. Reson. Med.*, vol. 58, no. 5, pp. 973–981, Nov. 2007.

[24] C. Liu, T. A. Bley, O. Wieben, J. H. Brittain, and S. B. Reeder, "Flow-independent T2-prepared inversion recovery black-blood MR imaging," *J. Magn. Reson. Imaging*, vol. 31, no. 1, pp. 248–254, 2010.

[25] S. M. van Heeswijk RB, Coppo S, Kober T, "High-Field MR Venography Using Adiabatic T2 Magnetization Preparation," *Proc. 19th Annu. ISMRM, Montr. Canada, 2011. (Abstract 1283).*, 2011.

[26] M. E. Andia *et al.*, "Flow-independent 3D whole-heart vessel wall imaging using an interleaved T2-preparation acquisition.," *Magn. Reson. Med.*, vol. 69, no. 1, pp. 150–7, Jan. 2013.

[27] C. Prieto *et al.*, "Highly efficient respiratory motion compensated free-breathing coronary mra using golden-step Cartesian acquisition," *J. Magn. Reson. Imaging*, vol. 41, no. 3, pp. 738–746, Feb. 2014.

[28] S. W. Atlas, R. I. Grossman, D. B. Hackney, H. I. Goldberg, L. T. Bilaniuk, and R. A. Zimmerman, "STIR MR imaging of the orbit," *Am. J. Roentgenol.*, vol. 151, no.

5, pp. 1025–1030, Nov. 1988.

[29] A. Haase, J. Frahm, W. Hänicke, and D. Matthaei W., *H-1-Nmr chemical-shift selective (CHESS) imaging*, vol. 30. 1985.

[30] P. G. Batchelor, D. Atkinson, P. Irarrazaval, D. L. G. Hill, J. Hajnal, and D. Larkman, "Matrix description of general motion correction applied to multishot images," *Magn. Reson. Med.*, vol. 54, no. 5, pp. 1273–1280, Nov. 2005.

[31] M. Modat *et al.*, "Fast free-form deformation using graphics processing units," *Comput. Methods Programs Biomed.*, vol. 98, no. 3, pp. 278–284, 2010.

[32] W. Kosiński, P. Michalak, and P. Gut, "Robust Image Registration Based on Mutual Information Measure," *J. Signal Inf. Process.*, vol. 3, no. 2, pp. 175–178, May 2012.

[33] R. R. Ingle *et al.*, "Nonrigid Autofocus Motion Correction for Coronary MR Angiography with a 3D Cones Trajectory," *Magn. Reson. Med.*, vol. 72, no. 2, pp. 347–361, Aug. 2014.

[34] D. Atkinson, D. L. G. Hill, P. N. R. Stoyle, P. E. Summers, and S. F. Keevil, "An autofocus algorithm for the automatic correction of motion artifacts in MR images BT - Information Processing in Medical Imaging," 1997, pp. 341–354.

[35] R. N. Bracewell, K.-. Chang, A. K. Jha, and Y.-. Wang, "Affine theorem for two-dimensional Fourier transform," *Electron. Lett.*, vol. 29, no. 3, p. 304, 1993.

[36] K. P. Pruessmann, M. Weiger, P. Börnert, and P. Boesiger, "Advances in sensitivity encoding with arbitrary k-space trajectories," *Magn. Reson. Med.*, vol. 46, no. 4, pp. 638–651, Oct. 2001.

[37] C. Forman, D. Piccini, R. Grimm, J. Hutter, J. Hornegger, and M. O. Zenge, "Reduction of respiratory motion artifacts for free-breathing whole-heart coronary MRA by weighted iterative reconstruction," *Magn. Reson. Med.*, vol. 73, no. 5, pp. 1885–1895, Jun. 2014.

[38] M. Weigel, "Extended phase graphs: Dephasing, RF pulses, and echoes - pure and simple," *J. Magn. Reson. Imaging*, vol. 41, no. 2, pp. 266–295, Feb. 2015.

[39] G. Captur *et al.*, "A medical device-grade T1 and ECV phantom for global T1

mapping quality assurance---the T1 Mapping and ECV Standardization in cardiovascular magnetic resonance (T1MES) program," *J. Cardiovasc. Magn. Reson.*, vol. 18, no. 1, p. 58, Sep. 2016.

[40] A. Etienne, R. M. Botnar, A. M. C. van Muiswinkel, P. Boesiger, W. J. Manning, and M. Stuber, "'Soap-Bubble' visualization and quantitative analysis of 3D coronary magnetic resonance angiograms," *Magn. Reson. Med.*, vol. 48, no. 4, pp. 658–666, Sep. 2002.

[41] K. Yoneyama, B. Ambale-Venkatesh, D. A. Bluemke, R. L. McClelland, and J. A.C. Lima, *Cardiovascular magnetic resonance in an adult human population: Serial observations from the multi-ethnic study of atherosclerosis*, vol. 19. 2017.

[42] S. Y. Ho and P. Nihoyannopoulos, "Anatomy, echocardiography, and normal right ventricular dimensions," *Heart*, vol. 92, no. Suppl 1, pp. i2–i13, Apr. 2006.

[43] L. Antiga, B. A. Wasserman, and D. A. Steinman, "On the overestimation of early wall thickening at the carotid bulb by black blood MRI, with implications for coronary and vulnerable plaque imaging," *Magn. Reson. Med.*, vol. 60, no. 5, pp. 1020–1028, Nov. 2008.

[44] M. Usman *et al.*, "Motion corrected compressed sensing for free-breathing dynamic cardiac MRI.," *Magn. Reson. Med.*, vol. 70, no. 2, pp. 504–16, Aug. 2013.

[45] T. Correia, G. Cruz, T. Schneider, R. M. Botnar, and C. Prieto, "Technical note: Accelerated nonrigid motion-compensated isotropic 3D coronary MR angiography," *Med. Phys.*, vol. 45, no. 1, pp. 214–222, Nov. 2017.

[46] A. Bustin *et al.*, "Five-minute whole-heart coronary MRA with sub-millimeter isotropic resolution, 100% respiratory scan efficiency, and 3D-PROST reconstruction," *Magn. Reson. Med.*, vol. 0, no. 0, Jul. 2018.

Captions

Figure 1 - Proposed iT2prep-IR sequence: a T2Prep-IR module is applied prior to data acquisition in odd heartbeats (bright-blood dataset for cardiac anatomy and lumen visualization) and no preparation is applied in even heartbeats. Fat suppression is achieved with a STIR like approach in odd dataset whereas SPIR is used in even dataset. Both odd and even datasets were acquired with a fully sampled spiral profile order Cartesian trajectory. 2D-iNAVs are acquired in each heartbeat to estimate/correct SI and RL translational motion. Non-rigid motion correction is performed on the two datasets and non-rigid image alignment is performed prior to dataset subtraction (black-blood dataset). T2prep=T2 preparation pulse, IR=inversion recovery pulse, TI=inversion time, iNAV=image navigator, SPIR=spectral pre-saturation inversion recovery pulse, ACQ=acquisition, SI: superior inferior, RL: left right.

Figure 2 - Simulation of the magnetization of the proposed iT2prep-IR sequence. The graphs show the magnetization of the myocardium (blue) and arterial blood (orange) in function of T2prep length for odd (MA), even (MB) and subtracted datasets (MB-MA) and the difference between myocardium and blood signal. Additionally, odd, even and subtracted magnetization are shown for the optimal T2prep length of 40ms. With a T2prep duration of 40ms the blood signal is well nulled in the subtracted dataset, whereas high myocardium to blood contrast in maintained in the bright-blood dataset.

Figure 3 - Magnetization evolution of blood (orange line) and myocardium (blue line) obtained from EPG simulations of the proposed iT2prep-IR (top) and previously proposed iT2prep approach (bottom) for a heart-rate of 45bpm. The yellow and purple rectangles show respectively the odd and even dataset acquired with the two sequences. Different graph scales were used to plot the iT2prep-IR and iT2prep magnetization to improve the visualization of the signal evolution for the two different approaches.

Figure 4 - Blood magnetization and myocardium-to-blood ratio of the direct subtracted volume obtained with the iT2prep and iT2prep-IR sequences for low (45bpm) and high (70bpm and 100bpm) heart rates. Better blood nulling and higher myocardium to blood ratio is obtained with the proposed approach for all simulated heart rates.

Figure 5 - Coronal and transversal views of bright and black blood iT2prep-IR images obtained for two representative healthy subjects. Aortic wall and RV wall are visible in the coronal views. RV, RA, LA and LV and aortic wall are visible in the transversal view. Good blood suppression was achieved for all cardiac chambers. RV: right ventricle, RA: right atrium, LA: left atrium, LV: left ventricle, Ao: aorta.

Figure 6 - a) Comparison of black-blood volumes obtained with DIR, iT2prep and iT2prep-IR sequences for two representative healthy subjects. LA, LV, RA and RV are visible, however some residual blood signal is present in DIR and iT2prep datasets (red arrows). b) Comparison of iT2prep and iT2prep-IR bright-blood volumes. Similar image quality is observed for both sequences. RV: right ventricle, RA: right atrium, LA: left atrium, LV: left ventricle, Ao: aorta.

Figure 7 - Top row: comparison of SNR_{myoc}, SNR_{blood} and $CNR_{myoc\text{-}blood}$ computed for bright and black-blood volumes acquired with DIR, iT2prep and iT2prep-IR sequences. The proposed sequence showed better results in terms of CNR in the black-blood volume and SNR of the myocardium. Bottom row: LA, LV, RA and RV wall thickness measurements obtained with DIR, iT2prep and iT2prep-IR sequences. No statistical difference is observed between iT2prep and the proposed sequence. DIR overestimates the wall thickness due to higher slice thickness used for the acquisition. RV: right ventricle, RA: right atrium, LA: left atrium, LV: left ventricle, Ao: aorta, ns=non-significant, * = $p<0.05$, ** = $p<0.01$, *** = $p<0.001$.

Figure 8 - Coronal and transversal views of bright and black blood iT2prep-IR images obtained for three representative patients. RV, RA, LA and LV and aortic wall are visible in the transversal view. Good blood suppression was achieved for all cardiac chambers. RV: right ventricle, RA: right atrium, LA: left atrium, LV: left ventricle. Average heart rates of the acquired patients were 62, 69, 71, 74 and 78bpm respectively.

Supporting Information Video S1 – bright-blood 3D volume acquired for one representative healthy subject.

Supporting Information Video S2 – co-registered black-blood 3D volume acquired for one representative healthy subject. Uniform blood suppression in obtained in all the cardiac chambers.

Supporting Information Figure 1 - Simulation of blood and myocardium magnetization obtained with different T2prep-IR module configurations (T2prep-IR or IR-T2prep). Blood and myocardium magnetizations were simulated for odd, even and subtracted datasets. No significant difference was observed between blood and myocardium magnetization obtained with the two approaches.

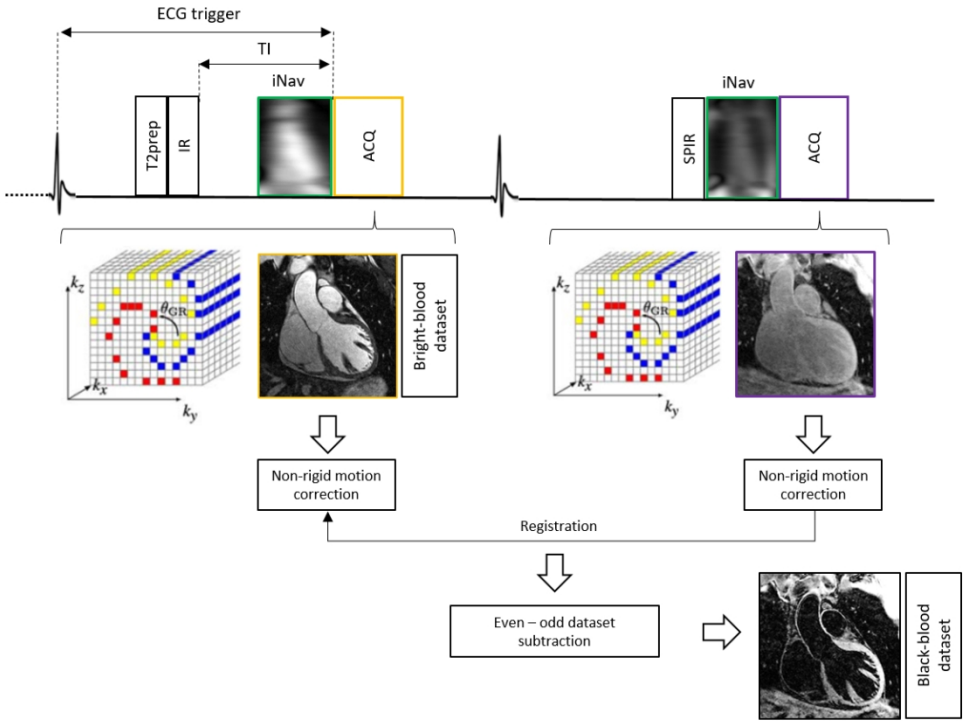

Figure 1 - Proposed iT2prep-IR sequence: a T2Prep-IR module is applied prior to data acquisition in odd heartbeats (bright-blood dataset for cardiac anatomy and lumen visualization) and no preparation is applied in even heartbeats. Fat suppression is achieved with a STIR like approach in odd dataset whereas SPIR is used in even dataset. Both odd and even datasets were acquired with a fully sampled spiral profile order Cartesian trajectory. 2D-iNAVs are acquired in each heartbeat to estimate/correct SI and RL translational motion. Non-rigid motion correction is performed on the two datasets and non-rigid image alignment is performed prior to dataset subtraction (black-blood dataset). T2prep=T2 preparation pulse, IR=inversion recovery pulse, TI=inversion time, iNAV=image navigator, SPIR=spectral pre-saturation inversion recovery pulse, ACQ=acquisition, SI: superior inferior, RL: left right.

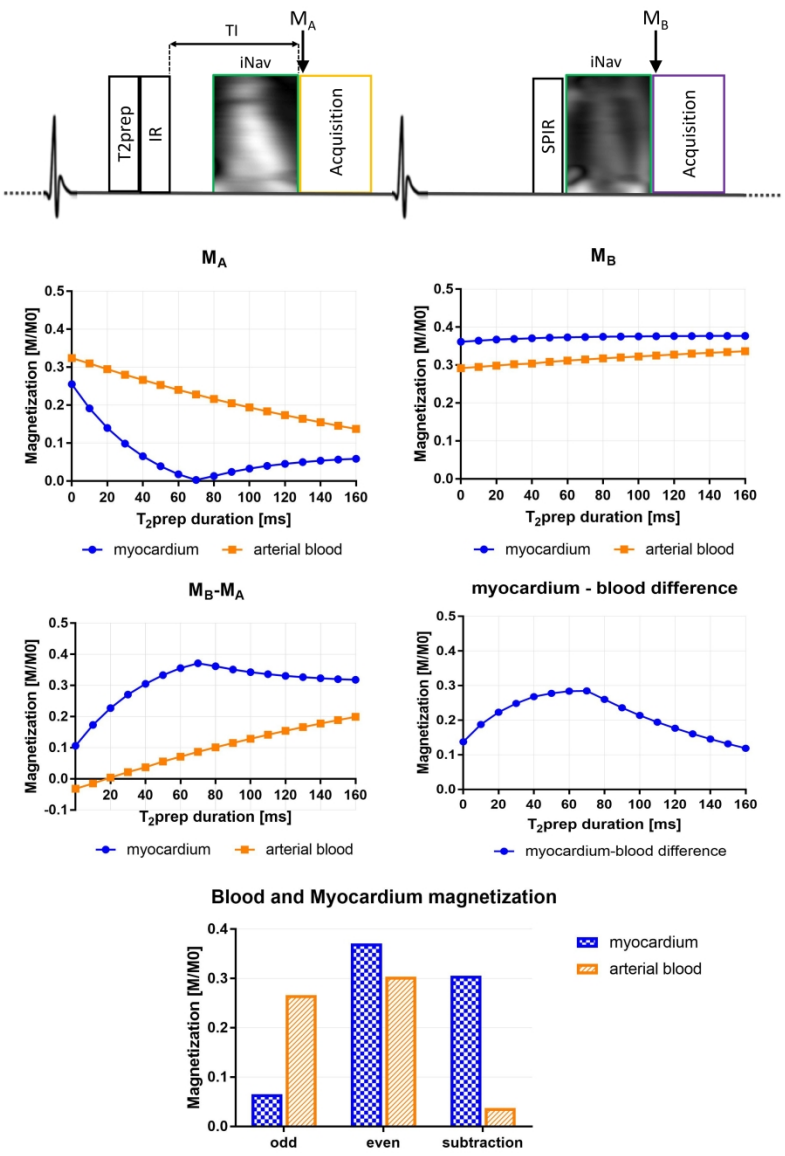

Figure 2 - Simulation of the magnetization of the proposed iT2prep-IR sequence. The graphs show the magnetization of the myocardium (blue) and arterial blood (orange) in function of T2prep length for odd (MA), even (MB) and subtracted datasets (MB-MA) and the difference between myocardium and blood signal. Additionally, odd, even and subtracted magnetization are shown for the optimal T2prep length of 40ms. With a T2prep duration of 40ms the blood signal is well nulled in the subtracted dataset, whereas high myocardium to blood contrast in maintained in the bright-blood dataset.

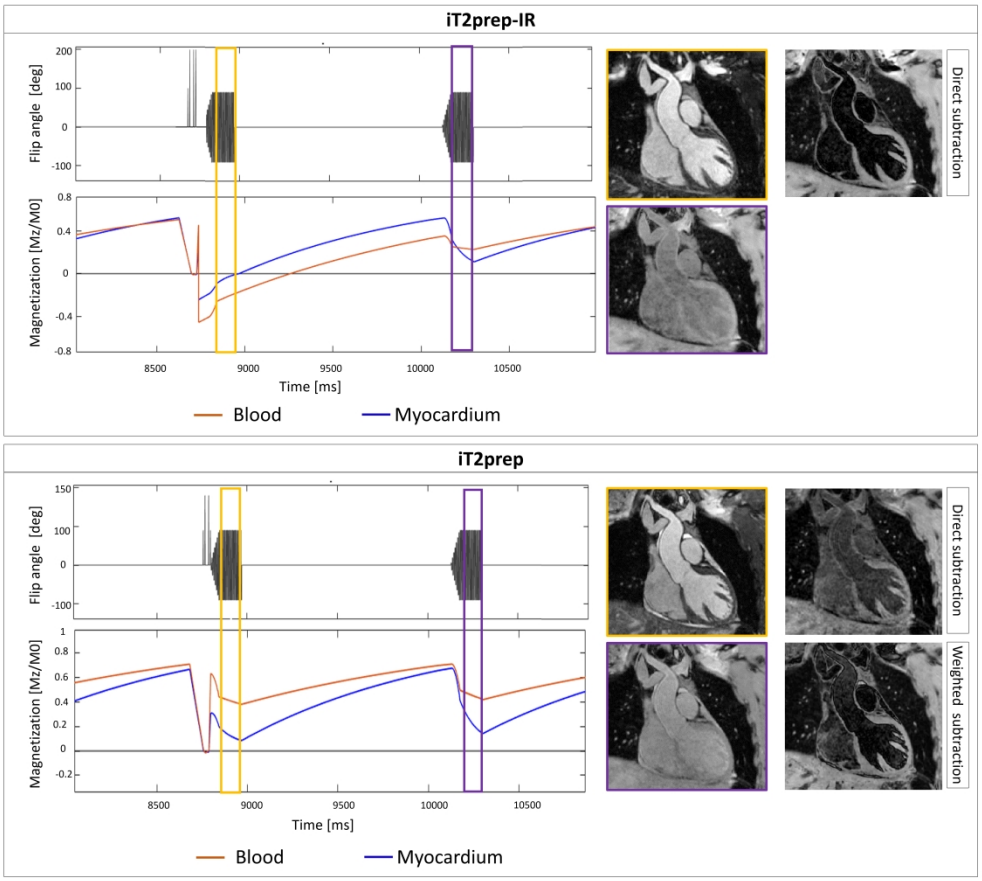

Figure 3 - Magnetization evolution of blood (orange line) and myocardium (blue line) obtained from EPG simulations of the proposed iT2prep-IR (top) and previously proposed iT2prep approach (bottom) for a heart-rate of 45bpm. The yellow and purple rectangles show respectively the odd and even dataset acquired with the two sequences. Different graph scales were used to plot the iT2prep-IR and iT2prep magnetization to improve the visualization of the signal evolution for the two different approaches.

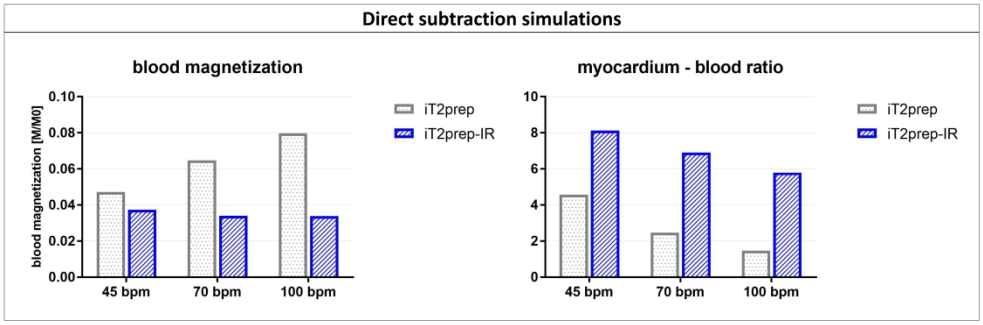

Figure 4 - Blood magnetization and myocardium-to-blood ratio of the direct subtracted volume obtained with the iT2prep and iT2prep-IR sequences for low (45bpm) and high (70bpm and 100bpm) heart rates. Better blood nulling and higher myocardium to blood ratio is obtained with the proposed approach for all simulated heart rates.

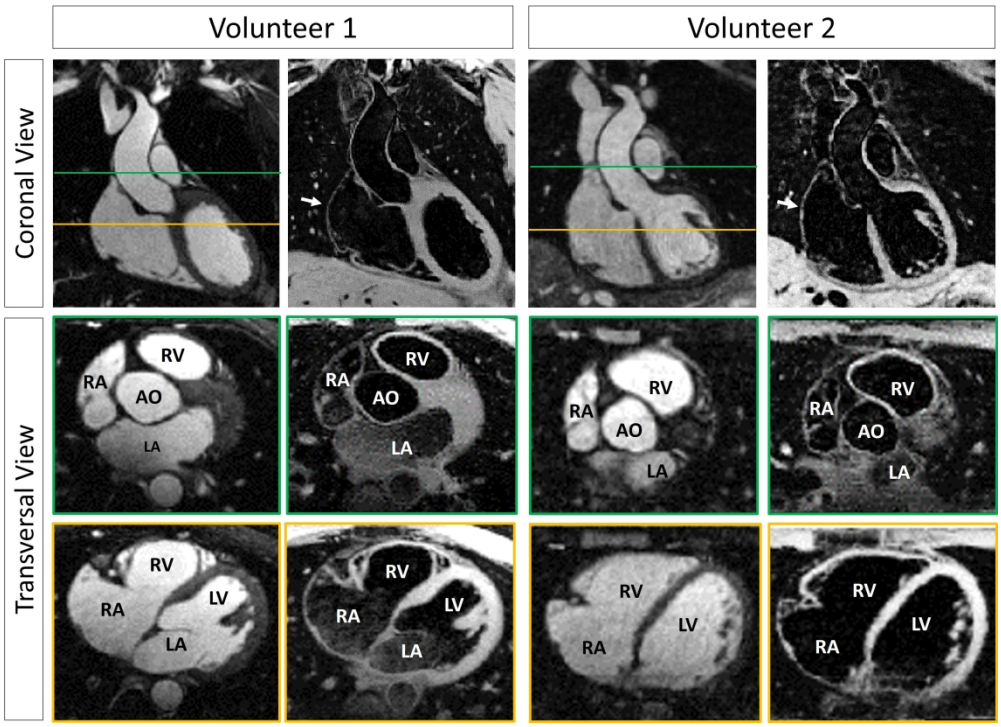

Figure 5 - Coronal and transversal views of bright and black blood iT2prep-IR images obtained for two representative healthy subjects. Aortic wall and RV wall are visible in the coronal views. RV, RA, LA and LV and aortic wall are visible in the transversal view. Good blood suppression was achieved for all cardiac chambers. RV: right ventricle, RA: right atrium, LA: left atrium, LV: left ventricle, Ao: aorta.

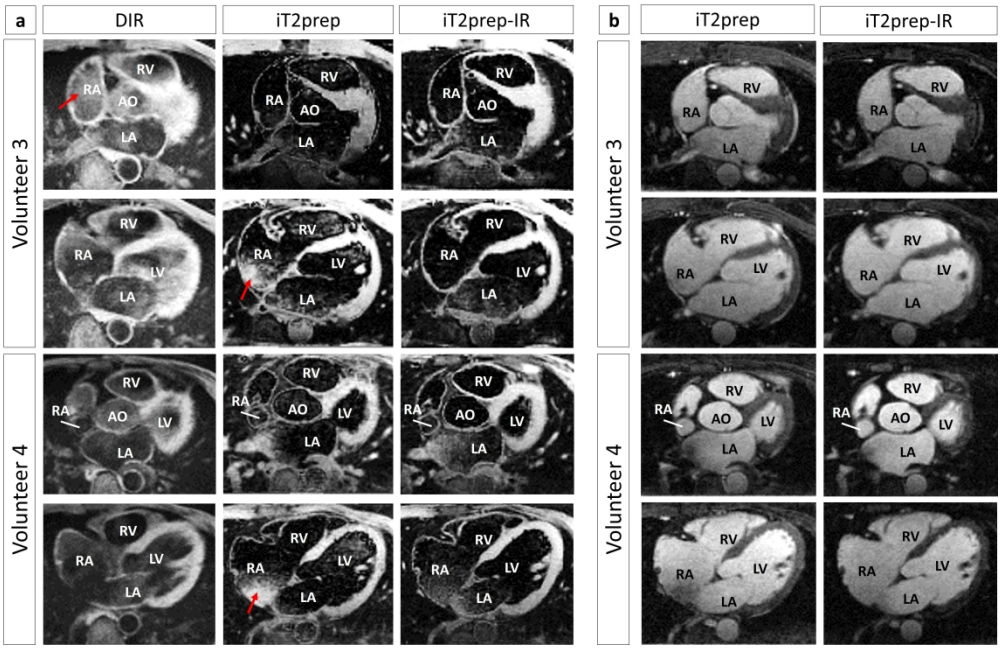

Figure 6 - a) Comparison of black-blood volumes obtained with DIR, iT2prep and iT2prep-IR sequences for two representative healthy subjects. LA, LV, RA and RV are visible, however some residual blood signal is present in DIR and iT2prep datasets (red arrows). b) Comparison of iT2prep and iT2prep-IR bright-blood volumes. Similar image quality is observed for both sequences. RV: right ventricle, RA: right atrium, LA: left atrium, LV: left ventricle, Ao: aorta.

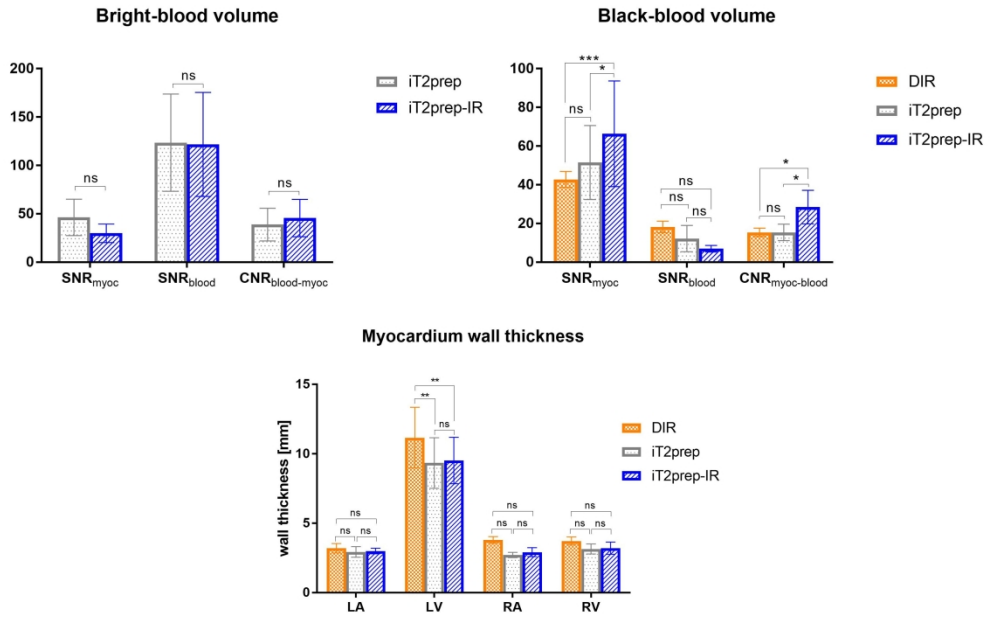

Figure 7 - Top row: comparison of SNRmyoc, SNRblood and CNRmyoc-blood computed for bright and black-blood volumes acquired with DIR, iT2prep and iT2prep-IR sequences. The proposed sequence showed better results in terms of CNR in the black-blood volume and SNR of the myocardium. Bottom row: LA, LV, RA and RV wall thickness measurements obtained with DIR, iT2prep and iT2prep-IR sequences. No statistical difference is observed between iT2prep and the proposed sequence. DIR overestimates the wall thickness due to higher slice thickness used for the acquisition. RV: right ventricle, RA: right atrium, LA: left atrium, LV: left ventricle, Ao: aorta, ns=non-significant, * = p<0.05, ** = p<0.01, *** = p<0.001.

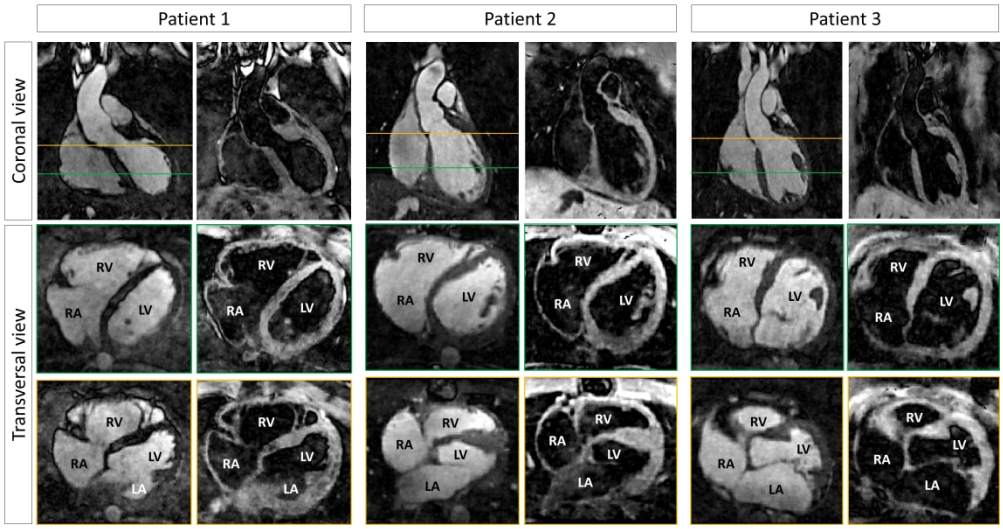

Figure 8 - Coronal and transversal views of bright and black blood iT2prep-IR images obtained for three representative patients. RV, RA, LA and LV and aortic wall are visible in the transversal view. Good blood suppression was achieved for all cardiac chambers. RV: right ventricle, RA: right atrium, LA: left atrium, LV: left ventricle. Average heart rates of the acquired patients were 62, 69, 71, 74 and 78bpm respectively.

Magnetization for different T2prep-IR configurations